An Improved Calculation of Proximity-Effect Loss in High-Frequency Windings of Round Conductors

Xi Nan and Charles R. Sullivan
xi.nan@dartmouth.edu charles.r.sullivan@dartmouth.edu http://engineering.dartmouth.edu/inductor
8000 Cummings Hall, Dartmouth College, Hanover, NH 03755, USA, Tel. +1-603-646-2851 Fax +1-603-646-3856

***Abstract*— The two best-known methods for calculating high-frequency winding loss in round-wire windings—the Dowell method and the Ferreira method—give significantly different results at high frequency. We apply 2-D finite-element method (FEM) simulations to evaluate the accuracy of each method for predicting proximity-effect losses. We find that both methods can have substantial errors, exceeding 60%. The Ferreira method, which is based on the exact Bessel-function solution for the eddy current in an isolated conducting cylinder subjected to a time-varying magnetic field, is found to be most accurate for loosely packed windings, whereas the Dowell method, which approximates winding layers comprising multiple turns of round wire with a rectangular conducting sheet, is most accurate for closely-packed windings.**

To achieve higher accuracy than is possible with either method alone, we introduce a new formula, based on modifying the Dowell method. Parameters in the new formula are chosen based on fitting our FEM simulation data. By expressing the results in terms of normalized parameters, we construct a model that can be used to determine proximity-effect loss for any round-wire winding with error under 2%.

***Index Terms*— proximity effect, winding loss**

I. Introduction

WINDING losses in transformers and inductors increase dramatically with frequency due to eddy-current effects. For design and optimization of inductors and transformers, there is an need for an accurate prediction of the winding losses over a wide frequency range and for various winding geometries. In this paper, we examine commonly used approximations for predicting winding losses in round-wire windings, show that they can have errors as large as 150%, and introduce a new method that provides much higher accuracy.

Commonly used methods to predict high-frequency loss in round-wire windings (reviewed in [1]) use one of two types of approximations to calculating AC conduction losses in windings of round conductors. The first approach is to replace the round conductors with square conductors of the same cross-sectional area and then substitute a conductor foil for the square conductors in the same layer, resulting in a one dimensional (1-D) model that can be solved analytically [2], [3], [4], [5], [6], [7]. This approach is commonly referred to as the Dowell method even though Dowell was not the first to employ it. The second approach is to use the well known Bessel function solution for the field in a cylindrical conductor [8], [9], [10]. We call this the Ferreira method because of Ferreira's work on practical application of this approach to windings [8], [11], [12]. The field solution used is exact for a single isolated cylinder placed in a uniform field. The primary approximation involved is the assumption that the losses remain unchanged when that cylinder is closely packed among other cylinders in a multi-turn winding. That approximation is partially overcome in [13], by considering the modification of the field in a conductor due to eddy current in adjacent conductors along the direction of the field. However, the approximation in [13] does not account for the effect of the distance to conductors in the other direction.

It is also possible to find the losses for any given configuration to any desired degree of accuracy by using numerical field solution methods such as the finite element method (FEM). Unfortunately, this remains impractical for many windings because fine wire and small skin depths require high-resolution meshes that are computationally expensive. In addition, the results of such a simulation typically provide information about only one specific design, and a large number of slow simulations would be required to optimize a design.

Several approaches have been used to overcome the limitations of direct numerical simulations. For situations in which the wire diameter is small compared to the skin depth ($d \ll \delta$), it is simple to perform an exact calculation of the losses in a wire given the ac field, and the ac field may be calculated from the terminal currents of the transformer and the inductor and a simple set of magnetostatic numerical field solutions [14]. This approach, called the squared-field-derivative (SFD) method, drastically reduces computation time, but it is only accurate for relatively low frequencies or for fine wire such as litz wire.

The idea of separating the analysis of the overall field shape from the analysis of the local interaction producing eddy currents is also applied in [15], but instead of the simple analytical calculation of eddy currents, [15] removes the limitation to ($d \ll \delta$) by performing a FEM simulation of the local field and eddy currents, using symmetry boundary conditions to approximate the periodic array of wires in a winding.

In this paper, we use a similar approach to [15], simulating a single wire with symmetry boundary conditions to find its behavior in a winding. However, instead of developing a system that repeats this simulation for each winding to be analyzed as in [15], we collect data for a range of wire spacings in two directions and for ratios of wire diameter to skin depth ranging from 0.6 to 60. We compare this data to calculations based

This work was supported in part by the United States Department of Energy under grant DE-FC36-01GO1106.

on the Dowell method and the Ferreira method to evaluate the accuracy and application range of these methods. We find that they both lead to error as large as or larger than 60% in some regions. Based on these results, we modify the Dowell method to provide a function that approximates the simulation results much better—to within 2%.

Section II reviews the Dowell method and the Ferreira method and shows normalized expressions for power loss with each of these two methods. Section III explains the setup of the model we used for 2-D FEM simulation. Section IV analyzes our results from the FEM simulation, and compares them with the results from the Dowell method and the Ferreira method. Section V provides a discussion of the use of a geometry factor of the winding called porosity factor included in previous literature [2], [8], [9], [16]. Section VI gives the form of our new function based on the 2-D simulation results.

II. The Dowell Method and the Ferreira Method

There are two kinds of eddy-current effects: Skin effect and proximity effect. When an ac current flows in a conductor, the current density tends to decrease from the surface to the center of the conductor and thus increase the power loss when the operating frequency gets high. This is called skin effect. The proximity effect is similar but it is caused by the current carried by a nearby conductor. The current in the nearby conductor causes a time-varying field and induces a circulating current inside the conductor. Both the skin effect and the proximity effect cause the current density to be nonuniform in the cross-section of the conductor and cause higher winding loss at higher frequency [17].

In this paper we focus exclusively on proximity-effect loss, because, in a multilayer winding, it strongly dominates over skin effect loss. Thus we examine the effect of an external AC field applied to a winding.

A. Proximity-Effect Factor

In this paper, proximity-effect losses are normalized and expressed with a unitless factor $\hat{G}$:

$$P = \hat{G}\frac{H^2}{\sigma} \tag{1}$$

where P is power loss per unit length; H is the peak value of the external sinusoidal magnetic field caused by currents in surrounding conductors; and σ is the conductivity of the conductor.

This definition (1) differs from some other definitions of G in that we normalize to conductor conductivity as well as applied field, such that $\hat{G}$ is unitless. This facilitates application of our results to any design, even with different conductor materials or temperatures.

B. Proximity Factor from the Dowell Method

In the Dowell method, a round conductor with diameter d is replaced by a square conductor of the same cross sectional area, with width equal to $\sqrt{\pi}d/2$. The expression for proximity effect loss per length of an infinite foil conductor with thickness $\sqrt{\pi}d/2$, can be obtained as a function of frequency [7]:

$$\hat{G} = \frac{P}{H^2}\sigma = \xi\frac{\sinh\xi - \sin\xi}{\cosh\xi + \cos\xi} \tag{2}$$

where ξ is defined as:

$$\xi = \frac{\sqrt{\pi}}{2}\frac{d}{\delta} \tag{3}$$

and δ is the skin depth, which is defined as:

$$\delta = \frac{1}{\sqrt{\pi f \mu \sigma}} \tag{4}$$

where μ and σ are the permeability and the conductivity of the conductor and f is the frequency of a sinusoidal current.

The skin effect losses of an infinite foil conductor with same width can be represented by the ratio of AC resistance to DC resistance as in [7]:

$$\frac{R_{ac}}{R_{dc}} = \frac{\xi}{2}\frac{\sinh\xi + \sin\xi}{\cosh\xi - \cos\xi} \tag{5}$$

Based on Dowell's assumptions and the general field solutions for the distribution of current density in a single layer of an infinitely long current sheet, the expression for the AC resistance of the mth layer is derived in [4], and is re-written in [8] as

$$R_{ac,m} = R_{dc,m}\frac{\xi}{2}\left[\frac{\sinh\xi + \sin\xi}{\cosh\xi - \cos\xi} + (2m-1)^2\frac{\sinh\xi - \sin\xi}{\cosh\xi + \cos\xi}\right] \tag{6}$$

where $R_{dc,m}$ is the DC resistance of a conductor in the winding; $R_{ac,m}$ is the AC resistance of a conductor in the winding; and m is the number of the layer under consideration.

Skin effect and proximity effect can be calculated separately due to the orthogonality existing between them [11]. Equation (6) can also be obtained from (5), (2) and the field assumption in [8].

Error is introduced in high frequencies by replacing round conductors with square conductors because substitution only results in the same DC resistance, while the approximation with the rectangular conductor underestimates the AC resistance at high frequency.

Dowell also introduced a porosity factor (also called layer factor) when converting the several conductors in a layer into one equivalent foil conductor to ensure the DC resistance of the model winding is the same as that of the original one. The porosity factor will be discussed in detail in Section V.

C. Proximity Factor of a Round Conductor

The exact expression for $\hat{G}$ based on an isolated round conductor is:

$$\hat{G} = -\frac{2\pi\gamma}{\gamma}\frac{ber_2\gamma ber'\gamma + bei_2\gamma ber'\gamma}{ber^2\gamma + bei^2\gamma} \tag{7}$$

in which

$$\gamma = \frac{1}{\sqrt{2}}\frac{d}{\delta} \tag{8}$$

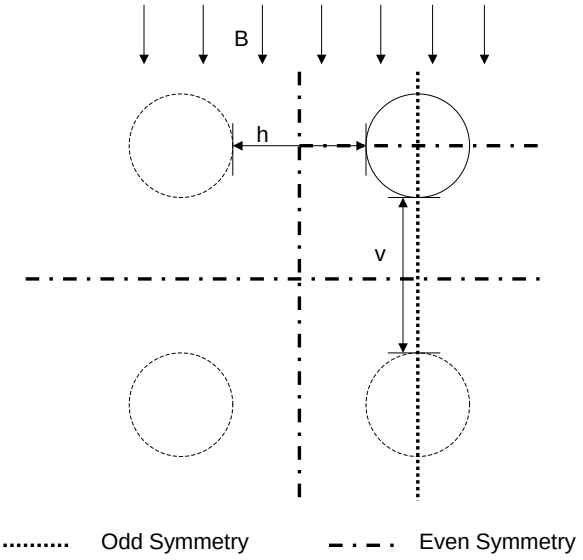

Fig. 1. 2-D simulation model for multilayer windings using symmetrical boundaries to simulate an infinite periodic array of turns. v is the interwire distance; h is the interlayer distance.

Ferreira applied the analytical field solution of a single isolated conductor to get an expression for the AC resistance of the mth layer by assuming a 1-D field inside the winding [8]. However, (7) doesn't represent how the distances between layers and conductors in multilayer windings affect power loss. It is only accurate for widely-spaced winding conductors, only in which case the interaction between conductors can be neglected.

III. 2-D Finite-Element Simulations for Multi-Layer Windings

To evaluate the accuracy of the Dowell method and the Ferreira method over a wide range of conditions, we performed FEM simulations for a 2-D model. Fig. 1 shows the model used to represent an infinite array of windings packed with a certain spacing defined by h (interlayer distance) and v (interwire distance).

Symmetric boundaries are used in this model as shown in Fig. 1. Even symmetric boundaries are set between layers and adjacent conductors in the same layer because of the geometry of the infinite array that we assume. Also, due to the symmetry of the current distribution in a round conductor in the infinite array with a uniform external field applied to it, an odd symmetric boundary can be set in the center of the conductor along the direction of the external field, and an even symmetric boundary can be set in the direction perpendicular to the external field. The net current in the conductor is set to zero so that the only current flowing in the conductor is that caused by the external field.

After solving the model by FEM with varying dimensions and frequencies, we found that power loss is a function of both the frequency and the dimensions. The normalized power loss $\hat{G}$ changes not only with frequency, but also with h/d and v/d, as shown in Fig. 2 and Fig. 3.

We performed a large number of simulations by sweeping these three variables: frequency, interlayer distance h, and interwire distance v. In our simulation, the frequency range is from 20 kHz to 2000 MHz with conductor diameter equal to 0.28 mm, corresponding to d/δ from 0.6 to 60. The range of dimensions is h/d from 0.26 to 1.8 (9 points) and v/d from 0.03 to 1.4 (10 points). A total of 3600 solutions have been acquired under all different combination of these three variables. The software we used for FEM simulation is a commercial package (Maxwell 2-D field simulator of Ansoft Corporation), and the target error of total field energy was set to 0.01%.

IV. Analysis of the Simulation Result

In Fig. 4, we compare the 2-D FEM simulation results with the results given by the Dowell method and the Ferreira method. Some significant conclusions can be drawn: First, in the low frequency range, the results from the Dowell method, the Ferreira method and the 2-D simulation are very close to each other. Second, the Dowell method underestimates proximity-effect loss at high frequency, while the Ferreira method overestimates it at high frequency. Third, the 2-D simulation results are closer to the Dowell method results when the conductors are more closely packed, while the Ferreira method is more accurate when the conductors are further apart.

Although it appears in Fig. 4 that the two models and the experimental results are equal in the low frequency region ($d \ll \delta$), the predictions of the Dowell and Ferreira methods differ by a factor of $\pi/3$, or 4.7%, in this region, due to the fact that the Dowell method chooses the size of the square conductor to match DC resistance, not proximity effect losses [18]. This difference is too small to be visible in the compressed log scale shown in Fig. 4, but closer examination of that data shows that the simulation results match the Ferreira method to about 1% in the region, and the Dowell method's prediction of low-frequency proximity effect loss has the expected error of about 5%.

Fig. 2 and 3 show examples of the relationship between power loss and geometry. Reducing the distance between conductors in the same layer or increasing the distance between layers can both reduce the proximity-effect loss. Proximity-effect loss at one specific frequency goes to a constant value which is consistent with that given by the Ferreira method when both v/d and h/d are well above one.

V. Some Discussion of the Porosity Factor

In the Dowell method, round-wire windings are converted into 'equivalent' foil conductors for easier analysis. The round wires are first replaced by square conductors of equal copper

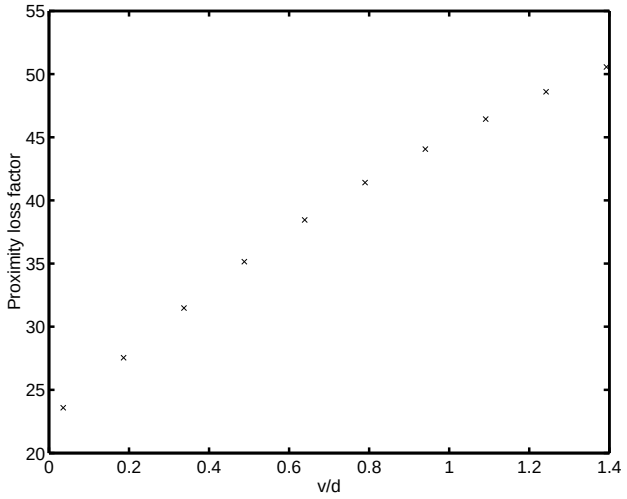

Fig. 2. Unitless normalized proximity-effect factor $\hat{G}$ versus normalized interwire spacing v/d with $d/\delta = 20.7$, and $h/d = 1.46$, where h is the interlayer distance and v is the interwire distance.

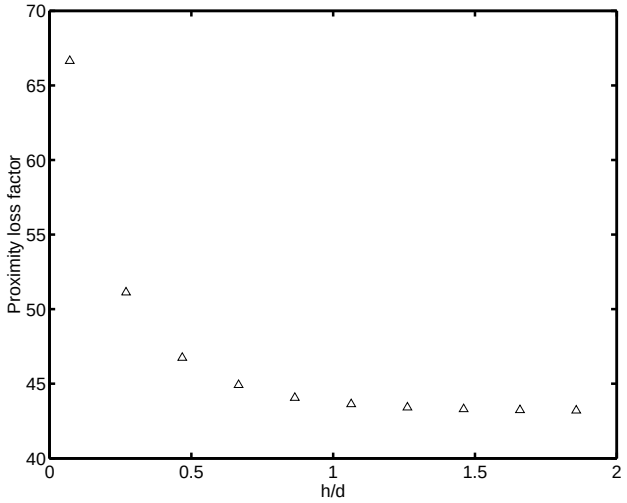

Fig. 3. Unitless normalized proximity-effect factor $\hat{G}$ versus normalized interlayer spacing h/d with $d/\delta = 20.7$, and $v/d = 0.9405$, where h is the interlayer distance and v is the interwire distance.

cross-sectional area. These square conductors are then brought together to form an equivalent foil winding. This foil winding of copper, which does not extend the entire window breath, is then "stretched" in the thickness direction to become a foil of equal height that does extend across the entire window breath. A layer porosity factor is introduced to match the DC resistance of the original winding. If N is the number of square conductors per layer, each having an individual width a, and b is the window width,

$$\eta = \frac{Na}{b} \tag{9}$$

Layer porosity factor was first introduced by Dowell [2]. In Dowell's model for porous layers, the current distribution change caused by the 1-D approximation is considered equivalent to a difference in the conductivity, and this difference is reflected by a $\sqrt{\eta}$ factor in the skin depth and thus in ξ. Thus the AC resistance in a winding of m layers can be derived from (6):

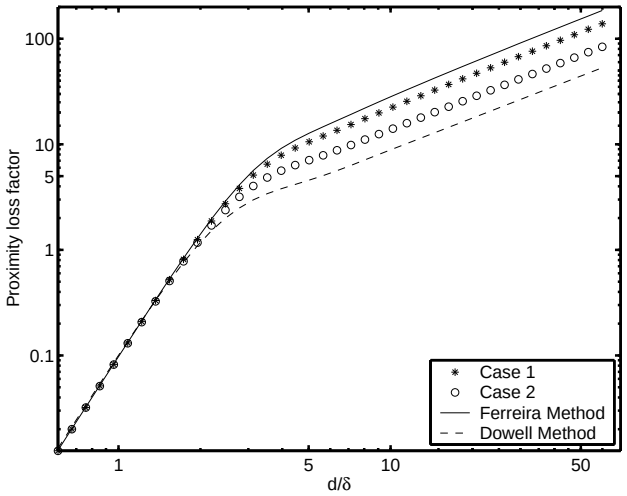

Fig. 4. 2-D FEM simulation result for unitless normalized proximity-effect factor $\hat{G}$ compared with results from the Dowell method and the Ferreira method (Case 1: h/d=1.86, v/d=1.24; Case 2: h/d=0.2698, v/d=0.1865).

$$R_{ac} = R_{dc}\xi'[\frac{\sinh 2\xi' + \sin 2\xi'}{\cosh 2\xi' - \cos 2\xi'} + \frac{2}{3}(m^2-1)\frac{\sinh 2\xi' - \sin 2\xi'}{\cosh 2\xi' + \cos 2\xi'} \tag{10}$$

where ξ' is defined as:

$$\xi' = \xi\sqrt{\eta} \tag{11}$$

However, it has been pointed out that, at high frequencies, the porosity factor only gives a good approximation when the conductors are closely packed [19], [16].

In [8], the magnetic field is compensated by a factor of η because the average current along the width of each layer is reduced by the same factor. Equation (10) becomes:

$$R_{ac} = R_{dc}\xi'[\frac{\sinh 2\xi' + \sin 2\xi'}{\cosh 2\xi' - \cos 2\xi'} + \eta^2\frac{2}{3}(m^2-1)\frac{\sinh 2\xi' - \sin 2\xi'}{\cosh 2\xi' + \cos 2\xi'} \tag{12}$$

We can derive an expression for $\hat{G}$ from (12) based on the 1-D field approximation in [8]

$$\hat{G} = \xi'\frac{\sinh \xi' - \sin \xi'}{\cosh \xi' + \cos \xi'} \tag{13}$$

Similarly, another expression for $\hat{G}$ can be derived from (10):

$$\hat{G} = \frac{1}{\eta^2}\xi'\frac{\sinh \xi' - \sin \xi'}{\cosh \xi' + \cos \xi'} \tag{14}$$

In [9], an η^2 factor is added to the Ferreira proximity-effect loss expression derived from the analytical solution of an isolated round conductor to compensate for the decrease of

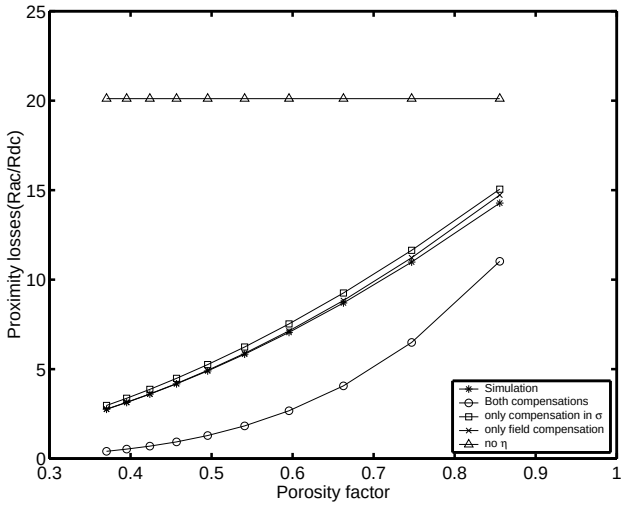

Fig. 5. Comparison of proximity-effect loss in 2-D simulation with various compensation methods with a porosity factor related to interwire distance v/d at low frequency where $d/\delta = 0.8368$ Comparison of proximity-effect loss in 2-D simulation with various compensation methods with a porosity factor related to interwire distance v/d with $d/\delta = 20.7$ and $h/d = 1.8571$ in the 6th layer of a multilayer winding.

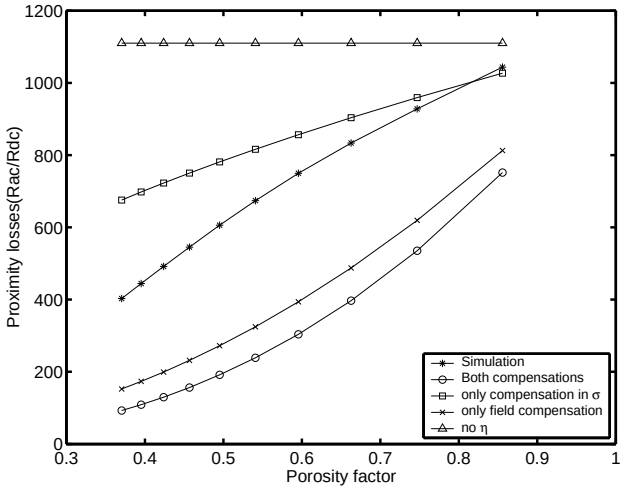

Fig. 6. Comparison of proximity-effect loss in 2-D simulation with various compensation methods with a porosity factor related to interwire distance v/d with $d/\delta = 20.7$ and $h/d = 1.8571$ in the 6th layer of a multilayer winding. This comparison shows that all of the methods in the literature entail substantial errors at high frequency.

magnetic field strength in a porous layer. But this η factor does not make any improvement to the Ferreira method in the aspect of taking the interaction between conductors into account since $\hat{G}$ in [9] is the same as in (7).

From our simulation results, $\hat{G}$ becomes smaller when v/d is reduced, while total proximity-effect losses become larger because of the increase of field strength when the conductors in the same layer comes closer together.

Fig. 5 and 6 compare the total proximity-effect loss from simulation results to the different compensations by η at different frequencies. From the two figures, we can see that when skin depth is of the same order as the width of the conductor, compensation of skin depth in (10) is accurate as stated in [20]. However, at a higher frequency, when the skin depth is much smaller than conductor width ($d/\delta = 20.7$), (10) is less accurate than it is at lower frequencies. Nonetheless, it can give better results than the other compensation methods, even though η is introduced to compensate the 2-D effects without rigorous justification [16].

From Fig. 7, we can see that the error of $\hat{G}$ in (14) can be from -20% to 60% compared with our simulation results. and in Fig. 8, the error of the Ferreira method can be up to 150% compared to the simulation result.

VI. Choosing the Functional Form for the Modified Dowell Method

Our aim is to create a function based on the data from 2-D simulations that can be directly used in calculating proximity-effect loss in multi-layer windings.

A new functional form is chosen based on the Dowell method, which is more frequently used and has a simpler form than the Ferreira method. Two coefficients k_1 and k_2 are added to the

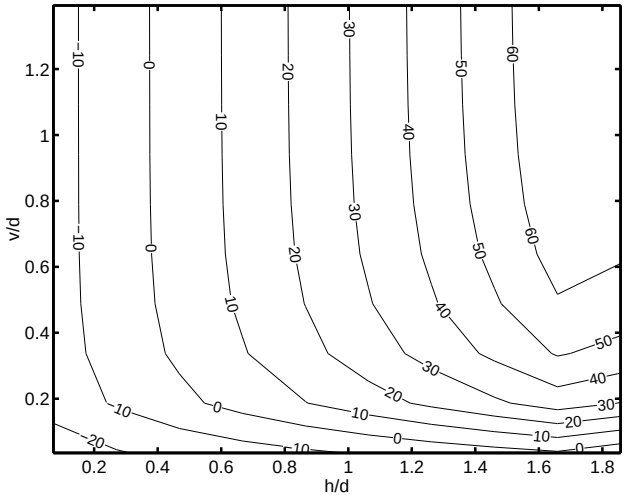

Fig. 7. Contour lines of error (%) in $\hat{G}$ from the Dowell method with porosity factor η (as in (14)), compared with simulation results at high frequency when d/δ=20.7 versus different interlayer distances h and interwire distances v.

Dowell function to better fit to the 2-D simulation results.

$$\hat{G}' = k_1\sqrt{k_2}X\frac{\sinh(\sqrt{k_2}X) - \sin(\sqrt{k_2}X)}{\cosh(\sqrt{k_2}X) + \cos(\sqrt{k_2}X)} \tag{15}$$

where X is defined as:

$$X = \frac{d}{\delta} \tag{16}$$

This approach of modifying the Dowell function based on FEM results, and indeed the form of the function (15), are similar to those in [21]. However, because we use it to find only $\hat{G}$, not an expression for AC resistance factor, the application of this formula is much more general than the modified Dowell function in [21], and, with the modifications discussed below, we achieve much higher accuracy.

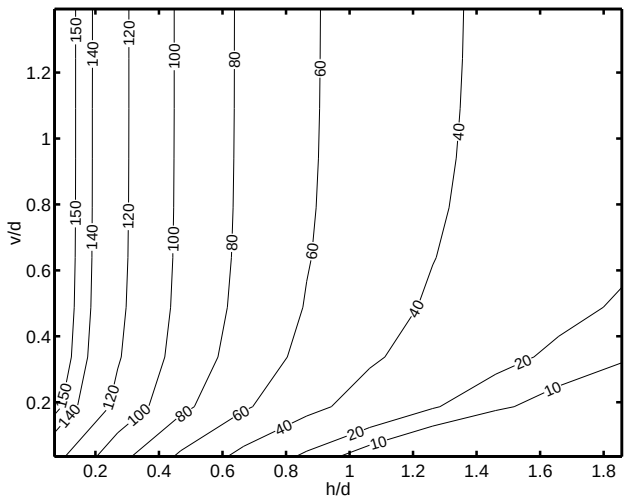

Fig. 8. Contour lines of percent error in $\hat{G}$ from the Ferreira method compared with simulation results at high frequency when $d/\delta = 20.7$ versus different interlayer distances h and interwire distances v.

When Dowell's function is modified by varying k_1 and k_2, the curve is scaled, but the shape is unchanged. Our simulation data, however, has a slightly different shape for different wire spacings. As shown in Fig. 9, the Dowell solution has a slight overshoot where the function transitions from the part of the of the curve that is proportional to ξ^4 (or f^2) to the part of the curve that is proportional to ξ (or $f^{0.5}$). The simulation data only exhibits this overshoot for small values of v/d. To produce a curve with the same general shape but without the overshoot, we introduce a new function:

$$\hat{d}(X) = \frac{KX}{(X^{-3n} + b^{3n})^{\frac{1}{n}}}. \tag{17}$$

This function is based on the curve-fit function used in [22], having two constant-slope portions, but is modified to have constant slopes of four and one on a log-log scale to fit the known high- and low-frequency asymptotic behavior of eddy currents. The constant b controls the point at which the transition between slopes occurs, and the constant n determines whether the transition is abrupt (large values of n) or smooth (small values of n). K is chosen to fit (17) to simulation data at low frequency, and from rough curve-fitting in the low frequency range, its value can be fixed at 0.0960.

As shown in Fig. 9, (17) provides a better fit for some geometries, whereas (15) provides a better fit for other geometries. To allow fitting data with either shape, or any intermediate shape, we used a weighted average of the two functions (15) and (17), with weighting w:

$$\hat{G}' = (1-w)k_1\sqrt{k_2}X\frac{\sinh(\sqrt{k_2}X) - \sin(\sqrt{k_2}X)}{\cosh(\sqrt{k_2}X) + \cos(\sqrt{k_2}X)} + w\hat{d}(X) \tag{18}$$

By fitting (18) to the 90 sets of data (in each set of data d/δ sweeps from 0.6 to 60 with 40 samples evenly distributed on a log scale), we obtained 90 sets of w, k_1, k_2, b, and n values, defining curves which fit the data from 2-D FEM simulations

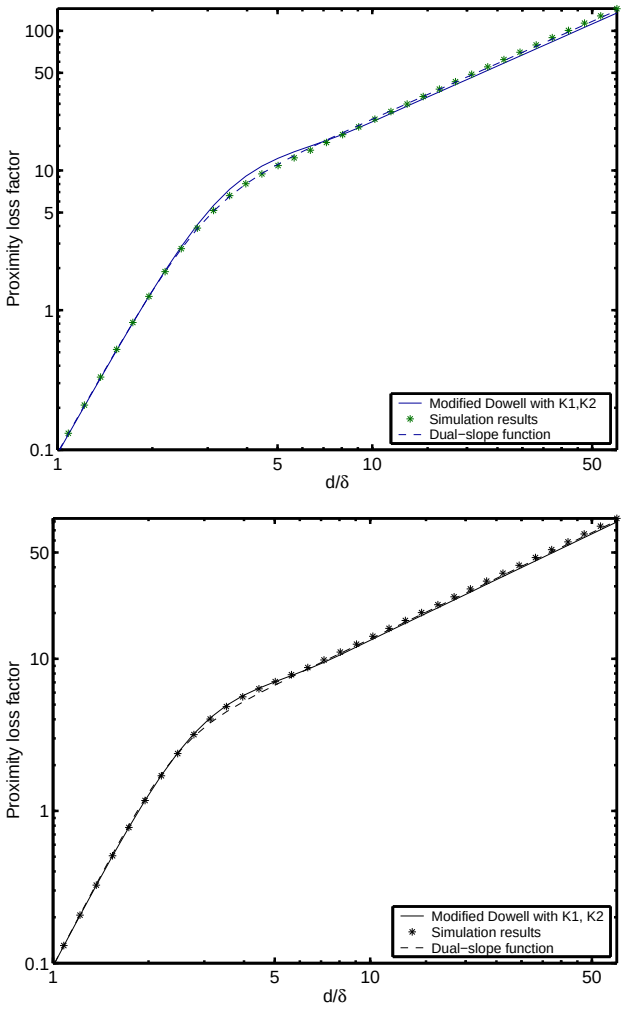

Fig. 9. Depending on geometry, the simulation results may or may not exhibit the "overshoot" in the Dowell function. In upper plot, simulation results for $h/d = 1.4603$ and $v/d = 0.1865$ are compared to the two curve fitting equations: the modified Dowell function (15) and the dual-slope function (17). In this case, the simulation data does not exhibit the overshoot and the dual-slope function (17) fits better. In the lower plot, data for $h/d = 0.2698$ and $v/d = 0.1865$ can be seen to be fit better by the modified Dowell function (15), although there is still significant error in the fit.

much better. Each set of values corresponds to a different v/d and h/d. Fig. 11 shows the error of our new function compared with the original 2-D simulation data, which is under 2% in all solutions for different dimension sets, and the only errors exceeding 1% occur at dimensional conditions of small h/d and large v/d, which are seldom used in practice.

To use the results we report above, one would look up the values of w, k_1, k_2, b, and n in Table I based on the values of v/d and h/d. We are presently studying different possible curve-fit functions that would give values of w, k_1, k_2, b, and n based on the values of v/d and h/d.

VII. Conclusion

In this paper, 2-D symmetrical numerical simulation results for the conductor loss in windings due to the proximity effect

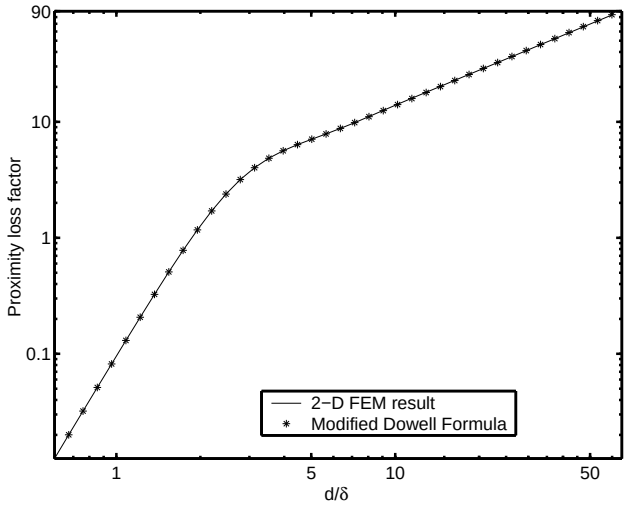

Fig. 10. Simulation results for $h/d = 0.2698$ and $v/d = 0.1865$ are compared to the combined curve fitting equation (18). The combined equation can be seen to fit the data better than is possible with either of the individual functions; this is the same data as in the second plot in Fig. 9.

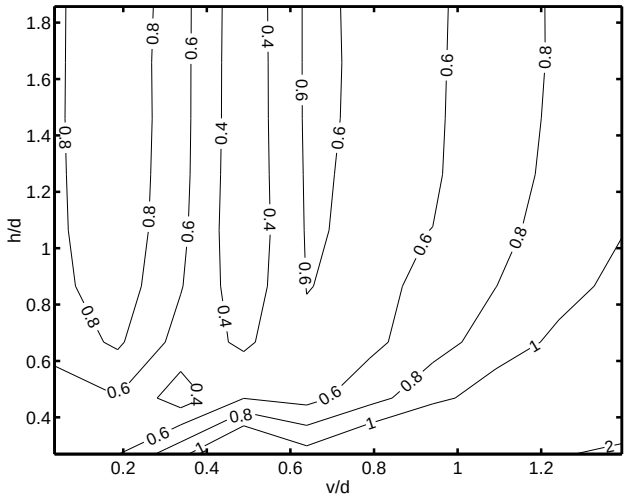

Fig. 11. Contour lines of maximum percent error for the curve fit (18) using the parameters in Table I for different dimensional conditions. The value associated with each contour line is the maximum percentage error over the frequency range tested, corresponding to values of d/δ from 0.6 to 60.

are presented. The result show that the Dowell method can have up to 60% error even with appropriate compensation by porosity factor and the Ferreira method can have up to 150% error. A new function which is based on the Dowell function has been chosen and it is shown to fit the 2-D simulation data with error under 2%.

REFERENCES

[1] Audrey M. Urling, Van A. Niemela, Glenn R. Skutt, and Thomas G.Wilson, "Characterizing high-frequency effects in transformer windings—a guide to several significant articles", *Journal of Circuits,Systems,and Computers*, vol. 5, no. spec issue, pp. 607–626, Dec. 1996.

[2] P.L. Dowell, "Effects of eddy currents in transformer windings", *Proceedings of the IEEE*, vol. 113, no. 8, pp. 1387–1394, Aug. 1966.

[3] P.S.Venkatraman, "Winding eddy current losses in switch mode power transformers due to rectangular wave currents", *Proceedings of Powercon 11,Power Concepts Inc.*, pp. 1–11, 1984.

[4] M.P. Perry, "Multiple layer series connected winding design for minimum losses", *IEEE Transactions on Power Apparatus and Systems*, vol. PAS-98, pp. 116–123, Jan./Feb. 1979.

[5] E.Bennet and S.C. Larson, "Effective resistance of alternating currents", *American Institute of Electrical Engineers*, vol. 59, pp. 1010–1017, 1940.

[6] Bruce Carsten, "High frequency conductor losses in switchmode magnetics", in *Technical Papers of the First International High Frequency Power Conversion 1986 Conference.*, May 1986, pp. 155–176.

[7] Richard L. Stoll, *The analysis of eddy currents*, Clarendon Press. Oxford, 1974.

[8] J. A. Ferreira, "Improved analytical modeling of conductive losses in magnetic components", *IEEE Transactions on Power Electronics*, vol. 9, no. 1, pp. 127–131, Jan. 1994.

[9] M.Bartoli, N. Noferi, and A. Reatti, "Modelling winding losses in high-frequency power inductors", *Journal of Circuits, Systems, and Computers*, vol. 5, no. spec issue, pp. 607–626, Dec. 1996.

[10] William R. Smythe, *Static and Dynamic Electricity*, McGraw-Hill, 1968, page 411.

[11] J. A. Ferreira, "Analytical computation of ac resistance of round and rectangular litz wire windings", *IEEE Proceedings-B Electric Power Applications*, vol. 139, no. 1, pp. 21–25, Jan. 1992.

[12] J. A. Ferreira, *Electromagnetic Modelling of Power Electronic Converters*, Kluwer Academic Publishers, 1989.

[13] J.Roudet J.P.Keradec, E. Laveuve, "Multipolar development of vector potential for parallel wires. application to the study of eddy currents effects in transformer windings", *IEEE transaction on Magnetics*, vol. 27, no. 5, pp. 4242 4245, 1991.

[14] Charles R. Sullivan, "Computationally efficient winding loss calculation with multiple windings, arbitrary waveforms, and two- or three-dimensional field geometry", *IEEE Transactions on Power Electronics*, vol. 16, no. 1, pp. 142–150, Jan. 2001.

[15] Alexander D. Podoltsev, "Analysis of effective resistance and eddy-current losses in multiturn winding of high-frequency magnetic components", *IEEE Transactions on Magnetics*, vol. 39, no. 1, pp. 539–548, Jan. 2003.

[16] F. Robert, "A theoretical discussion about the layer copper factor used in winding losses calculation", *IEEE Transactions on Magnetics*, vol. 38, no. 5, pp. 3177–3179, Sept. 2000.

[17] P. N. Murgatroyd, "Calculation of proximity losses in multistranded conductor bunches", *IEEE Proceedings, Part A*, vol. 36, no. 3, pp. 115–120, 1989.

[18] Charles R. Sullivan, "Optimal choice for number of strands in a litz-wire transformer winding", *IEEE Transactions on Power Electronics*, vol. 14, no. 2, pp. 283–291, 1999.

[19] E. C. Snelling, *Soft Ferrites, Properties and Applications*, Butterworths, second edition, 1988.

[20] J.P Schauwers F. Robert, P. Mathys, "Ohmic losses calculation in SMPS transformers: Numerical study of Dowell's approach accuracy", *IEEE Transactions on Magnetics*, vol. 34, no. 4, pp. 1255–1257, July 1998.

[21] J.P Schauwers F. Robert, P. Mathys, "A closed-form formula for 2-d ohmic losses calculation in smps transformer foils", *IEEE Transactions on Power Electronics*, vol. 16, no. 2, pp. 437–444, May 2001.

[22] S.R. Sanders C.R. Sullivan, "Models for induction machines with magnetic saturation of the main flux path", *IEEE Transactions on Industry Applications*, vol. 31, no. 4, pp. 907–17, 1995.

TABLE I

VALUES OF k_1, k_2, b, n, w BASED ON NORMALIZED INTERWIRE DISTANCE v/d AND NORMALIZED INTERLAYER DISTANCE h/d

	$h/d=$ 1.8571	$h/d=$ 1.6587	$h/d=$ 1.4603	$h/d=$ 1.2619	$h/d=$ 1.0635	$h/d=$ 0.8651	$h/d=$ 0.6667	$h/d=$ 0.4683	$h/d=$ 0.2698
$v/d=1.3929$	k_1=2.6428	k_1=2.6478	k_1=2.6558	k_1=2.6695	k_1=2.6933	k_1=2.7348	k_1=2.8092	k_1=2.9501	k_1=3.2451
	k_2=0.4701	k_2=0.4696	k_2=0.4689	k_2=0.4677	k_2=0.4656	k_2=0.4620	k_2=0.4558	k_2=0.4447	k_2=0.4238
	b=0.1835	b=0.1831	b=0.1825	b=0.1815	b=0.1799	b=0.1770	b=0.1720	b=0.1628	b=0.1447
	n=1.0000	n=1.0000	n=1.0000	n=1.0000	n=1.0000	n=1.0000	n=1.0000	n=1.0000	n=1.0000
	w=0.0405	w=0.0404	w=0.0403	w=0.0402	w=0.0400	w=0.0395	w=0.0387	w=0.0371	w=0.0335
$v/d=1.2421$	k_1=2.5709	k_1=2.5743	k_1=2.5805	k_1=2.5910	k_1=2.6099	k_1=2.6440	k_1=2.7065	k_1=2.8274	k_1=3.0852
	k_2=0.4766	k_2=0.4763	k_2=0.4757	k_2=0.4747	k_2=0.4730	k_2=0.4699	k_2=0.4644	k_2=0.4543	k_2=0.4346
	b=0.1885	b=0.1883	b=0.1877	b=0.1869	b=0.1853	b=0.1825	b=0.1774	b=0.1678	b=0.1485
	n=1.0000	n=1.0000	n=1.0000	n=1.0000	n=1.0000	n=1.0000	n=1.0000	n=1.0000	n=1.0000
	w=0.0411	w=0.0410	w=0.0409	w=0.0408	w=0.0405	w=0.0398	w=0.0388	w=0.0367	w=0.0322
$v/d=1.0913$	k_1=2.4883	k_1=2.4900	k_1=2.4942	k_1=2.5017	k_1=2.5164	k_1=2.5430	k_1=2.5937	k_1=2.6950	k_1=2.9158
	k_2=0.4844	k_2=0.4843	k_2=0.4839	k_2=0.4832	k_2=0.4817	k_2=0.4792	k_2=0.4744	k_2=0.4653	k_2=0.4471
	b=0.1951	b=0.1950	b=0.1945	b=0.1938	b=0.1923	b=0.1896	b=0.1843	b=0.1742	b=0.1532
	n=1.0000	n=1.0000	n=1.0000	n=1.0000	n=1.0000	n=1.0000	n=1.0000	n=1.0000	n=1.0000
	w=0.0420	w=0.0420	w=0.0419	w=0.0418	w=0.0413	w=0.0406	w=0.0393	w=0.0365	w=0.0309
$v/d=0.9405$	k_1=2.3905	k_1=2.3918	k_1=2.3948	k_1=2.4002	k_1=2.4099	k_1=2.4297	k_1=2.4697	k_1=2.5516	k_1=2.7362
	k_2=0.4943	k_2=0.4942	k_2=0.4938	k_2=0.4933	k_2=0.4923	k_2=0.4903	k_2=0.4862	k_2=0.4783	k_2=0.4616
	b=0.2047	b=0.2046	b=0.2042	b=0.2034	b=0.2020	b=0.1993	b=0.1937	b=0.1825	b=0.1591
	n=1.0000	n=1.0000	n=1.0000	n=1.0000	n=1.0000	n=1.0000	n=1.0000	n=1.0000	n=1.0000
	w=0.0441	w=0.0441	w=0.0439	w=0.0437	w=0.0432	w=0.0423	w=0.0404	w=0.0367	w=0.0295
$v/d=0.7897$	k_1=2.2762	k_1=2.2766	k_1=2.2785	k_1=2.2820	k_1=2.2888	k_1=2.3029	k_1=2.3320	k_1=2.3955	k_1=2.5452
	k_2=0.5066	k_2=0.5066	k_2=0.5064	k_2=0.5060	k_2=0.5052	k_2=0.5036	k_2=0.5004	k_2=0.4937	k_2=0.4787
	b=0.2190	b=0.2191	b=0.2187	b=0.2179	b=0.2164	b=0.2134	b=0.2072	b=0.1942	b=0.1667
	n=1.0000	n=1.0000	n=1.0000	n=1.0000	n=1.0000	n=1.0000	n=1.0000	n=1.0000	n=1.0000
	w=0.0482	w=0.0483	w=0.0481	w=0.0477	w=0.0470	w=0.0457	w=0.0430	w=0.0377	w=0.0282
$v/d=0.6389$	k_1=2.1444	k_1=2.1446	k_1=2.1455	k_1=2.1473	k_1=2.1511	k_1=2.1595	k_1=2.1785	k_1=2.2241	k_1=2.3413
	k_2=0.5221	k_2=0.5221	k_2=0.5220	k_2=0.5217	k_2=0.5213	k_2=0.5202	k_2=0.5179	k_2=0.5124	k_2=0.4991
	b=0.2424	b=0.2423	b=0.2419	b=0.2413	b=0.2397	b=0.2362	b=0.2287	b=0.2121	b=0.1772
	n=1.0000	n=1.0000	n=1.0000	n=1.0000	n=1.0000	n=1.0000	n=1.0000	n=1.0000	n=1.0000
	w=0.0572	w=0.0572	w=0.0570	w=0.0566	w=0.0557	w=0.0536	w=0.0494	w=0.0408	w=0.0271
$v/d=0.4881$	k_1=2.0447	k_1=2.0450	k_1=2.0454	k_1=2.0465	k_1=2.0489	k_1=2.0545	k_1=2.0676	k_1=2.0993	k_1=2.1824
	k_2=0.5341	k_2=0.5340	k_2=0.5340	k_2=0.5338	k_2=0.5335	k_2=0.5328	k_2=0.5311	k_2=0.5270	k_2=0.5166
	b=0.1700	b=0.1699	b=0.1698	b=0.1696	b=0.1691	b=0.1679	b=0.1650	b=0.1579	b=0.1394
	n=2.0000	n=2.0000	n=2.0000	n=2.0000	n=2.0000	n=2.0000	n=2.0000	n=2.0000	n=2.0000
	w=0.0108	w=0.0108	w=0.0107	w=0.0107	w=0.0107	w=0.0106	w=0.0103	w=0.0097	w=0.0081
$v/d=0.3373$	k_1=1.8443	k_1=1.8445	k_1=1.8446	k_1=1.8451	k_1=1.8463	k_1=1.8493	k_1=1.8569	k_1=1.8768	k_1=1.9328
	k_2=0.5624	k_2=0.5624	k_2=0.5624	k_2=0.5623	k_2=0.5621	k_2=0.5617	k_2=0.5605	k_2=0.5575	k_2=0.5491
	b=0.1918	b=0.1918	b=0.1917	b=0.1915	b=0.1909	b=0.1894	b=0.1857	b=0.1760	b=0.1508
	n=2.0000	n=2.0000	n=2.0000	n=2.0000	n=2.0000	n=2.0000	n=2.0000	n=2.0000	n=2.0000
	w=0.0109	w=0.0109	w=0.0109	w=0.0109	w=0.0108	w=0.0107	w=0.0103	w=0.0093	w=0.0070
$v/d=0.1865$	k_1=1.6194	k_1=1.6128	k_1=1.6127	k_1=1.6131	k_1=1.6136	k_1=1.6151	k_1=1.6193	k_1=1.6314	k_1=1.6669
	k_2=0.6002	k_2=0.6015	k_2=0.6015	k_2=0.6014	k_2=0.6013	k_2=0.6010	k_2=0.6002	k_2=0.5980	k_2=0.5914
	b=0.2213	b=0.2285	b=0.2285	b=0.2281	b=0.2274	b=0.2253	b=0.2196	b=0.2038	b=0.1646
	n=2.0000	n=2.0000	n=2.0000	n=2.0000	n=2.0000	n=2.0000	n=2.0000	n=2.0000	n=2.0000
	w=0.0100	w=0.0117	w=0.0117	w=0.0117	w=0.0116	w=0.0113	w=0.0105	w=0.0087	w=0.0055
$v/d=0.0357$	k_1=1.3557	k_1=1.3556	k_1=1.3556	k_1=1.3556	k_1=1.3556	k_1=1.3563	k_1=1.3578	k_1=1.3639	k_1=1.3831
	k_2=0.6559	k_2=0.6559	k_2=0.6559	k_2=0.6560	k_2=0.6559	k_2=0.6558	k_2=0.6554	k_2=0.6539	k_2=0.6491
	b=0.2529	b=0.2529	b=0.2530	b=0.2529	b=0.2526	b=0.2500	b=0.2435	b=0.2217	b=0.1668
	n=2.0000	n=2.0000	n=2.0000	n=2.0000	n=2.0000	n=2.0000	n=2.0000	n=2.0000	n=2.0000
	w=0.0086	w=0.0086	w=0.0086	w=0.0086	w=0.0086	w=0.0083	w=0.0078	w=0.0060	w=0.0031